Theor Appl Climatol
DOI 10.1007/s00704-013-0919-8

ORIGINAL PAPER

Spatial patterns and temporal trends of precipitation in Iran

Tayeb Raziei · Jamal Daryabari · Isabella Bordi · Luis S. Pereira

Received: 8 July 2012 / Accepted: 23 April 2013

Abstract Spatial patterns of monthly, seasonal and annual precipitation over Iran and the corresponding long-term trends for the period 1951–2009 are investigated using the Global Precipitation Climatology Centre gridded dataset. Results suggest that the spatial patterns of annual, winter and spring precipitation and the associated coefficients of variation reflect the role of orography and latitudinal extent between central-southern arid and semi-arid regions and northern and western mountainous areas. It is also shown that precipitation occurrence is almost regularly distributed within the year in northern areas while it is more concentrated in a few months in southern Iran. The spatial distribution of Mann–Kendal trend test (Z statistics) for annual precipitation showed downward trend in north-western and south-eastern Iran, whereas western, central and north-eastern exhibited upward trend, though not statistically significant in most regions. Results for winter and autumn revealed upward trend in most parts of the country, with the exception of north-western and south-eastern where a downward trend is observed; in spring and summer, a downward trend seems to prevail in most of Iran. However, for all seasons the areas where the detected trend is statistically significant are limited to a few spot regions. The overall results suggest that the precipitation is decreasing in spring and summer and increasing in autumn and winter in most of Iran, i.e. less precipitation during the warm season with a consequent intensification of seasonality and dryness of the country. However, since the detected trends are often not statistically significant, any stringent conclusion cannot be done on the future tendencies.

T. Raziei
Soil Conservation and Watershed Management Research Institute (SCWMRI), Tehran, Iran

J. Daryabari
Department of Geography, Azad University of Semnan, Semnan, Iran
e-mail: mohit.map@gmail.com

I. Bordi
Department of Physics, Sapienza University of Rome, Rome, Italy
e-mail: isabella.bordi@roma1.infn.it

T. Raziei (✉) · L. S. Pereira
CEER-Biosystems Engineering, Institute of Agronomy, Technical University of Lisbon, Lisbon, Portugal
e-mail: tayebrazi@yahoo.com

L. S. Pereira
e-mail: lspereira@isa.utl.pt

1 Introduction

Precipitation is highly variable in space and time as it is the end product of complex interactions between a variety of dynamic processes with characteristic spatial and temporal scales. The space–time variability of precipitation plays a key role in water resource management and water allocation, particularly in regions characterised by arid and semi-arid climates. In recent years, interest has increased in learning about precipitation variability and trend in order to improve predictability for periods from months to years, important for agricultural purposes and climate studies, respectively. According to IPCC (2007), during recent decades, precipitation has tended to increase in mid-latitudes, decrease in the Northern Hemisphere subtropical zones, and increase generally throughout the Southern Hemisphere. Lettenmaier et al. (1994), Turkes (1996), Zhang et al. (2000), González Hidalgo et al. (2003), Gong et al. (2004) and Partal and Kahya (2006) are some of the researchers who have investigated recent rainfall trends in different geophysical fields.

Due to the complex orography (Fig. 1a) and wide latitudinal extent—from the descending branch of the Hadley cell up to mid-latitudes—precipitation in Iran is highly variable both in space and time (Raziei et al. 2012). Precipitation occurrences and amounts vary from the Caspian region and the relatively humid western and northern mountainous areas to the arid and semi-arid regions of central and eastern Iran, where sporadic precipitation events occur. This suggests that Iran has several precipitation regimes as identified

Published online: 08 May 2013

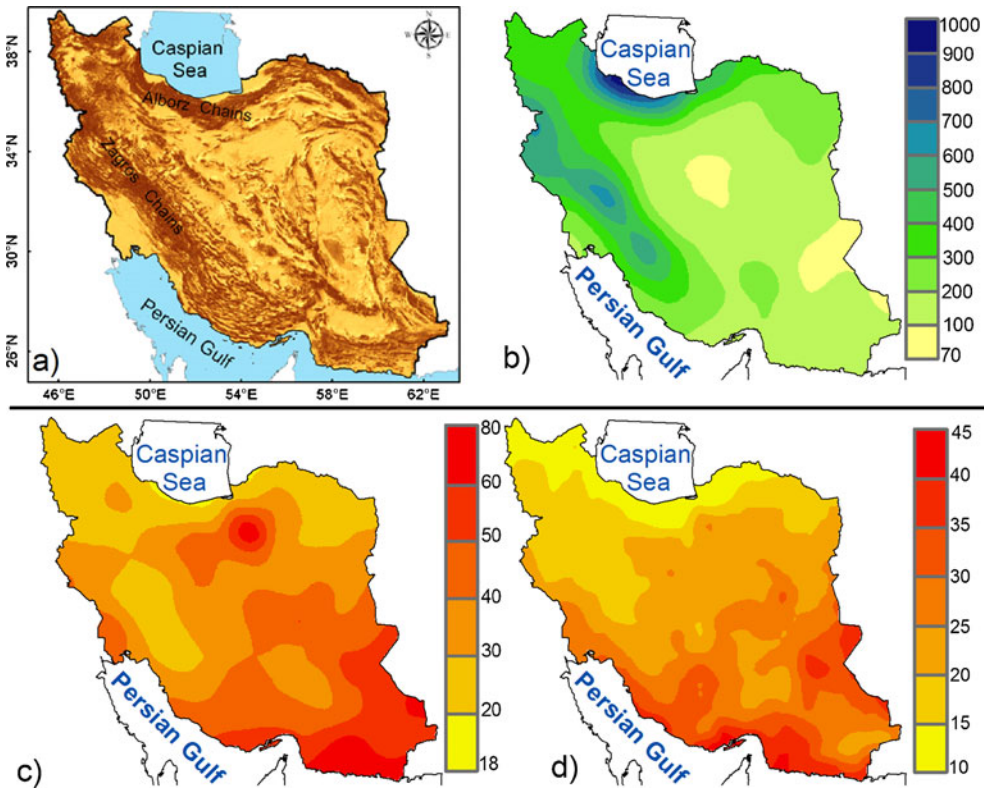

Fig. 1 Topography map of Iran (**a**), spatial pattern of annual total precipitation in millimetres (**b**) and respective CV in per cent (**c**); PCI, non-dimensional (**d**)

in previous studies, e.g. Domroes et al. (1998), Dinpashoh et al. (2004), Soltani et al. (2007) and Raziei et al. (2008). Recently, Raziei et al. (2012) have identified the spatial modes of the seasonal regime of daily precipitation over Iran using the APHRODITE gridded precipitation dataset for the Middle East (Yatagai et al. 2008, 2009) with a spatial resolution of 0.5°. The regional modes of variability were identified with the S-mode principal component analysis and Varimax rotation, applied to the subset of days when at least 10 % of all grid-points over Iran received precipitation of ≥5 mm. For autumn and winter, Iran has divided into five precipitation regimes, while for spring four precipitation regimes were identified.

Concerning the climate variability and trend analysis of the meteorological variables, several studies have been undertaken for Iran but mainly focusing on some specific regions rather than the whole country. Raziei et al. (2005) tested annual precipitation trend in central-eastern arid and semi-arid regions of Iran for the period 1965–2000 and showed no evidence of climate change. Modarres and da Silva (2007) analysed the time series of annual rainfall, annual number of rainy days and monthly rainfall in the same regions and also found a not statistically significant variability. Modarres and Sarhadi (2009) investigated the temporal variability and trends in annual total precipitation and 24-h maximum precipitation and showed that the annual rainfall is decreasing at 67 % of the Iranian stations, mostly in northern and north-western Iran, while the 24-h maximum rainfall is increasing at 50 % of the stations which are mostly located in arid and semi-arid regions. More recently, Tabari and Hosseinzadeh Talaee (2011) studied the annual and seasonal precipitation trends for 41 Iranian meteorological stations for the period 1966–2005 using the Mann–Kendall test, the Sen's slope estimator and the linear regression. Their results indicated a decreasing trend in annual precipitation at about 60 % of the stations from which seven stations were statistically significant with downward trends mostly occurring in the northwest of Iran, thus in agreement with findings of Modarres and Sarhadi (2009).

It can be noticed that existing studies either focus on specific regions or considered very sparse stations throughout the country. Thus, the main objective of this study is to analyse the spatial patterns of monthly, seasonal and annual total precipitation in Iran and to investigate their long-term trends using the Global Precipitation Climatology Centre (GPCC) gridded precipitation dataset with 0.5° resolution (Schneider et al. 2008). The dataset has already passed a very careful quality control and is temporarily long enough (1951–2009) for performing trend analysis. Therefore, it is expected that the present study can provide a more reliable and comprehensive spatial analysis of monthly, seasonal and annual precipitation variability and trends over the target area.

The introduction is followed by Section 2 that describes the GPCC dataset and the Mann–Kendal trend test used in the study. Section 3 is devoted to the description of results

and discussion on trend analysis. Finally, conclusions are presented in Section 4.

2 Data and methods

2.1 Data

The latest version of GPCC precipitation dataset for the period 1951–2009 with 0.5° spatial resolution is used for the analysis. The GPCC Full Data Product Version 5, updated in December 2010, is a gauge-based gridded monthly precipitation dataset for the global land surface, available in 2.5-, 1-, and 0.5-grid resolutions. The dataset covers the period 1901–2009 and is based on both non-real-time and real-time stations (Schneider et al. 2008). GPCC monthly precipitation analysis products are based on anomalies from climatological normals at the stations, or from GPCC high-resolution gridded climatology where no station normal is available. The anomalies are spatially interpolated by the analysis method of Spheremap (Willmott et al. 1985), and the gridded anomalies are then superimposed on the GPCC climatology 2010. The new GPCC precipitation climatology (reference period, 1951–2000) consists of normals collected by WMO, delivered by the countries to GPCC or calculated from time series of monthly data (with at least ten complete years of data) available in the GPCC data base (for details see the GPCC annual reports at http://gpcc.dwd.de). Recently, Raziei et al. (2010, 2011) have assessed the spatial and temporal variability of drought over Iran using the GPCC Full Data Product Version 4 (previous version), finding good and satisfactory agreement with observations and NCEP/NCAR reanalysis, respectively.

To assess the monthly, seasonal and annual precipitation spatial variability and trends over Iran, only grid points representative of Iran (630 grids) were considered. Seasons from winter to autumn are defined as: December–January–February (DJF), March–April–May (MAM), June–July–August (JJA) and September–October–November (SON).

2.2 Methods

The Precipitation Concentration Index (PCI), which is an intra-annual precipitation variability index (De Luis et al. 2000) defined as the ratio of the accumulated monthly squared precipitation to the squared annual precipitation, is computed for all grid points over Iran. The index ranges from less than 10, when monthly rainfall distribution over the year is quite uniform, to values above 20, corresponding to climates with substantial monthly variability in rainfall amounts and large concentration of the precipitation in a few months of the year (De Luis et al. 2000). As a measure of the annual and seasonal precipitation variability in relation to the mean, the coefficient of variation (CV) has been computed at each grid point. The CV is given by the standard deviation divided by the mean and multiplied by 100, i.e. it expresses the standard deviation as a percentage of the sample mean.

Two types of trends including monotonic trend and step (shift) change are usually considered for climatological and hydrological variables (Xu et al. 2003). For trend analysis, the null hypothesis $H0$ is that there is no trend in the population from which the dataset is drawn while $H1$ implies that there is a trend in the record. Non-parametric tests are usually more robust compared with parametric ones, among which the Mann–Kendall test is the most used in hydrology and climatology. Therefore, to detect any monotonic trends in the precipitation time series at all considered grid points, the Mann–Kendall test was used. This test consists of comparing each value of the time series with the remaining in a sequential order. The S statistic is the sum of all the counting given by Eq. (1) (da Silva 2004):

$$S = \sum_{i=1}^{n-1} \sum_{k=i+1}^{n} \operatorname{sign}(x_k - x_i) \tag{1}$$

where x_k and x_i are the sequential data values, n is the length of the dataset and sign (θ) is equal to 1, 0 or −1 when θ is greater than, equal to or less than zero, respectively. A very high positive value of S is an indicator of an increasing trend, while a very low negative value indicates a decreasing trend. The normalized Z statistics can be computed as:

$$Z = \begin{cases} \frac{S-1}{\sqrt{\mathrm{Var}(S)}} & \text{if } S > 0 \\ 0 & \text{if } S = 0 \\ \frac{S+1}{\sqrt{\mathrm{Var}(S)}} & \text{if } S < 0 \end{cases} \tag{2}$$

where Var(S) is:

$$\mathrm{Var}(S) = \frac{1}{18}\left[n(n-1)(2n+5) - \sum_{p=1}^{q} t_p(t_p-1)(2t_p+5)\right] \tag{3}$$

where q is the number of tied groups (a tied group is a set of sample data having the same value), and t_p is the number of data points in the pth group. Thus, the probability associated with this normalized test statistics can be easily computed; the significant probability level of 0.95 was applied, and p values were obtained for each analysed time series. The trend is said to be decreasing if Z is negative and the computed probability is greater than the level of significance while it is increasing if Z is positive and the computed probability is greater than the level of significance. If the computed probability is less than the level of significance, there is no trend.

3 Results

3.1 Spatial patterns of precipitation

Figure 1b, c depicts the spatial patterns of total annual precipitation and the corresponding CV over Iran, respectively. The spatial pattern of total annual precipitation reflects the role of orography, sea neighbourhood and sharp elevation differences between central arid and semi-arid areas and northern and western mountainous regions in precipitation distribution over Iran. The highest total annual precipitation is observed in the Caspian Sea region and mountainous areas of northern and western Iran while the lowest is observed in the central, eastern and southern Iran. The highest precipitation in the Caspian Sea region is due to the closeness of the sea to the high Alborz Mountains that enhances the land-sea interaction (condensation barrier effect), causing high and regularly distributed precipitation over the region all through the year. Over the mountainous areas of western Iran, there is a second maximum of annual precipitation, again related to the effect of orography in enhancing the precipitation processes, particularly windward of the Zagros Mountain. In the lee side of the Zagros and Alborz chains, there is a vast area (central-eastern Iran) where precipitation amounts are quite low (arid or semi-arid region). This is also confirmed by the spatial pattern of the CV of the annual total precipitation, showing the lowest values in the northern country and the highest (about 80 %) in the central-southern Iran, having high inter-annual variation that makes water resources management difficult. An important desert of Iran is in the southern foothill of Alborz, the Dashte-Kavir desert, which is well represented in Fig. 1c as an isolated area with very high CV values.

The spatial pattern of PCI is shown in Fig. 1d. It depicts substantial differences between northern and southern Iran with respect to the distribution of precipitation along the year. The lowest PCI values, ranging from 10 to 15, are in northern Iran, close to the Caspian Sea, which suggest that this area has relatively regular precipitation distribution throughout the year, whereas the mountainous areas of western and north-eastern Iran, with PCI values ranging from 15 to 20, are characterised by noticeable seasonality. PCI values rapidly increase from the foothills of Alborz and Zagros mountains to the southern and eastern Iran, showing a very sharp gradient, featuring central, southern and eastern Iran with substantial seasonality in precipitation (Fig. 1d). In this vast area PCI>20, especially in the southernmost and eastern Iran, denoting a concentration of most of annual total precipitation in a few months of the year. The spatial pattern of PCI is very similar to that of CV in Fig. 1c, suggesting that the areas characterised by substantial seasonality in precipitation (high PCI) have more variable and less predictable precipitation occurrences. Differently, the very low PCI values in Fig. 1d well correspond to areas characterised by low CV (Fig. 1c), so featuring the northern and north-western Iran with more regular precipitation occurrences.

The spatial patterns of seasonal precipitation and their CV over Iran are shown in Fig. 2. The spatial patterns for DJF and MAM seasons are relatively similar to that of annual total precipitation (Fig. 1b). Results characterise northern and western mountainous regions with the highest precipitation and central, eastern and southern Iran with the lowest ones. The highest precipitation (350–400 mm) in DJF is observed over western Iran while during MAM both western and northern mountainous regions receive relatively identical precipitation amounts. The JJA and SON are very dry seasons, particularly in central, eastern and southern Iran. In both seasons, the highest precipitation is observed in mountainous areas of Alborz and in the Caspian Sea region, with noticeable amounts of 120–140 mm in JJA and 350–400 mm in SON. The monsoon precipitation that usually occurs in the arid region of south-eastern Iran is well captured by JJA map as an isolated precipitation core with a value of about 20–40 mm of precipitation. The central and southern Iran is usually dry in summer, leaving this vast area with less than 20 mm of precipitation in average. However, during SON, western Iran receives noticeable precipitation (50–100 mm) when compared with the JJA season.

Maps of CV for DJF and SON characterise northern Iran, along the Caspian Sea and Alborz Mountain, as an area with less than 40 % of CV. In MAM season, the CV increases all over the country with the maximum value observed in south-eastern Iran (about 150 %). The map of CV for JJA implies that the precipitation variability is extremely high all over Iran; the exception is the coastal areas of the Caspian Sea that commonly receive considerable precipitation in summer. It is worth noting that particularly high values of CV are due to the very low mean precipitation during summer.

The spatial patterns of month-to-month variations of precipitation over Iran are displayed in Fig. 3. The spatial patterns of precipitation in December, January, February and March are very similar to the pattern of DJF in Fig. 2; these show that the highest precipitation amount occurs in the mountainous areas of western Iran and the lowest are in the central, eastern and southern regions. Precipitation maps from April to September well display the retreatment of precipitation pattern from south to north, being restricted only to the Caspian Sea region in August and September. The Monsoon precipitation advancement and the influenced area (south-eastern Iran) is also well represented in the maps of June to August with the highest impact in June, that in average produces about 15–20 mm of precipitation. Maps

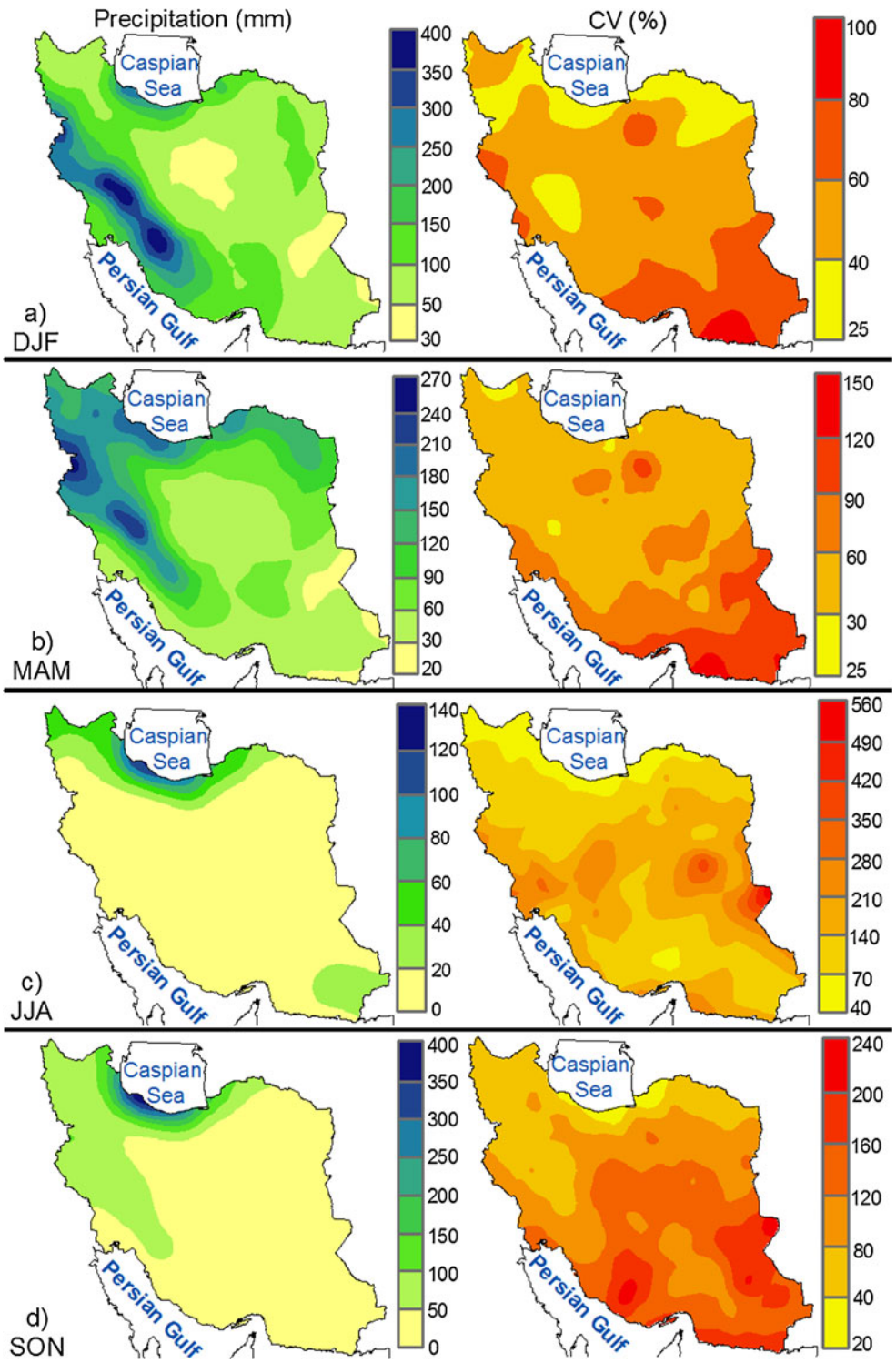

Fig. 2 Spatial patterns of seasonal precipitation in millimetres (*left*) and their CVs (*right*) for winter (**a**), spring (**b**), summer (**c**) and autumn (**d**) in per cent

suggest that the observed maximum precipitation in winter months (about 100–160 mm), which usually occurs in western Iran (Fig. 3a–c), is comparable to the maximum autumnal precipitation occurring in the Caspian Sea region (Fig. 3j–l). Differently, the maximum spring precipitation occurs in north-western Iran (Fig. 3e, f).

3.2 Trend analysis

The spatial pattern of MK trend test for total annual precipitation is presented in Fig. 4. Downward trends are found in north-western and south-eastern Iran, whereas western, central and north-eastern areas are

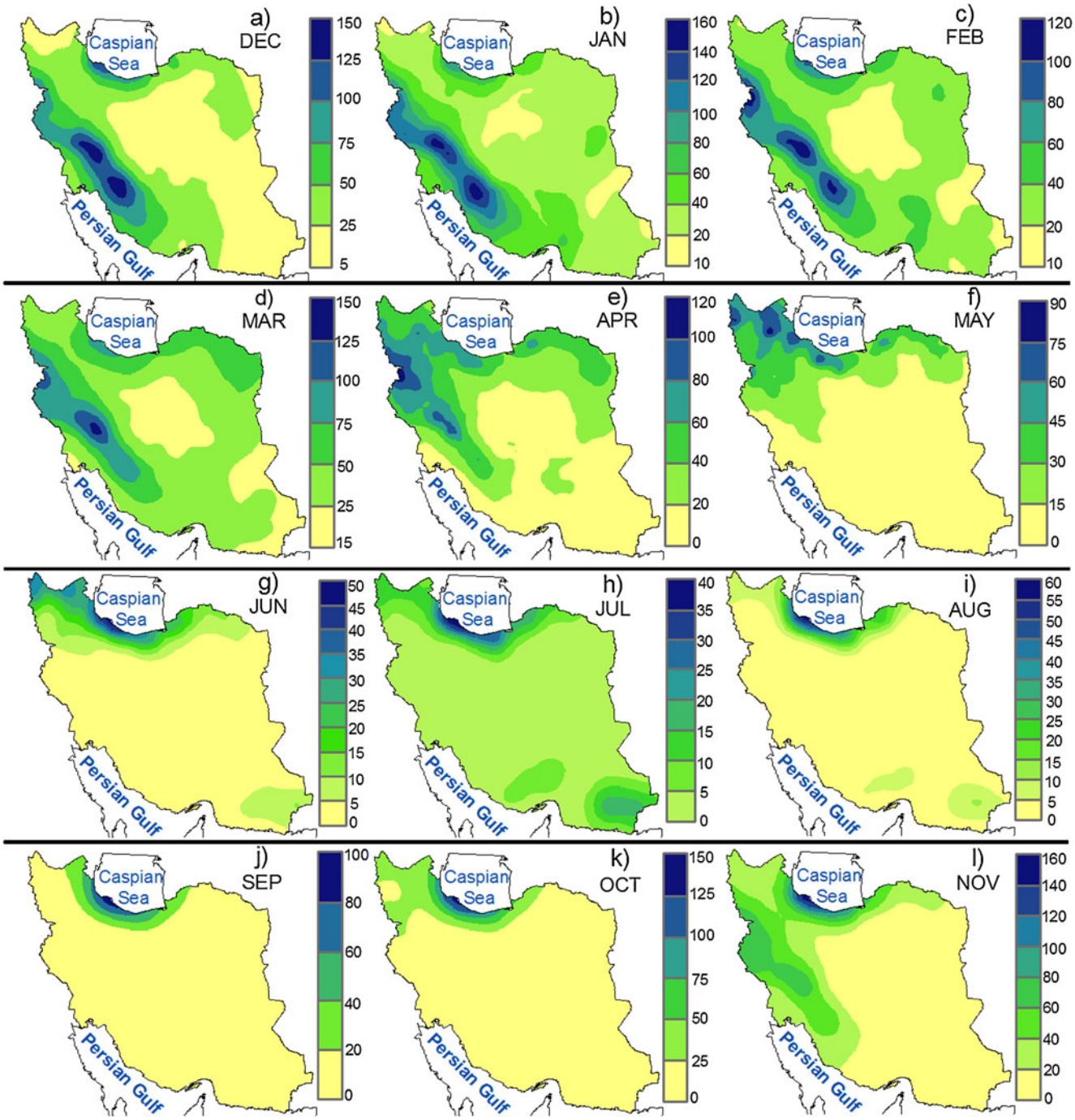

Fig. 3 Month-to-month variation in spatial pattern of precipitation (in millimetres) over Iran

characterised by upward trends. The observed downward trend is statistically significant whereas the upward trend is statistically significant only in some spot areas in south-western and central Iran. Results agree with those from Modarres and da Silva (2007), Modarres and Sarhadi (2009) and Tabari and Hosseinzadeh Talaee (2011) using observation data.

The spatial patterns of MK trend test for each season are displayed in Fig. 5. Figure 5a suggests that the winter precipitation is increasing in most regions, particularly in northern Iran where the trend is statistically significant. However, similar to annual precipitation, winter precipitation exhibits downward trend in north-western and south-eastern Iran, though it is not statistically significant. Differently, Fig. 5b shows that spring precipitation tends to decrease in most of Iran, bounding the upward trend into the central-western Iran detected for winter. That observed downward trend is statistically significant in north-western and eastern

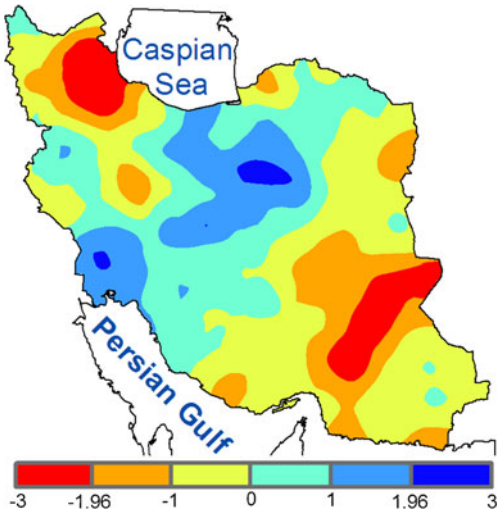

Fig. 4 Spatial pattern of Mann–Kendal trend test (Z statistics) for annual precipitation over Iran. Statistically significant upward and downward trends are for $Z \geq 1.96$ and $Z \leq -1.96$, respectively

Iran. The spatial pattern of MK trend for JJA displays also not statistically significant downward trends in most parts of Iran, particularly in southern and western Iran. Similarly to the winter season, the precipitation during SON (Fig. 5d) shows upward trend in most of Iran, whereas the downward trend is limited to north-western and south-eastern regions; however, these trends are not statistically significant.

Generally, precipitation in SON and DJF shows upward trend in most parts of Iran, with the exception of north-western and south-eastern country, where the observed trend is downward in both seasons. Nevertheless, again trends are not statistically significant. On the contrary, the target area is mostly characterised by downward trend in MAM and JJA, with the exception of limited areas in central and north-eastern Iran, which show upward trends. Thus, it seems that in most of the country precipitation tends to decrease during the warm seasons (MAM and JJA) and increase during the cold seasons (SON and DJF). Therefore, using the GPCC dataset it seems that the climate in Iran is expected to become dryer than at the present, with substantial seasonality in many regions. Furthermore, it appears that the statistically significant trends in DJF and MAM seasons are responsible for the long-term trends observed in the annual precipitation (Fig. 4).

The spatial patterns of MK trend test for each month are shown in Fig. 6. The months from June to September have been excluded since they are very dry months in most of Iran, and therefore it is difficult to properly detect long-term trends in the related time series. Figure 6a shows that precipitation in December tends to increase in central-northern and decrease in south and north-western Iran. With the exception of limited areas in south-eastern, north-western and north-eastern Iran, the whole country exhibits upward trend in January, however generally not statistically significant. In February, most parts of the country show not

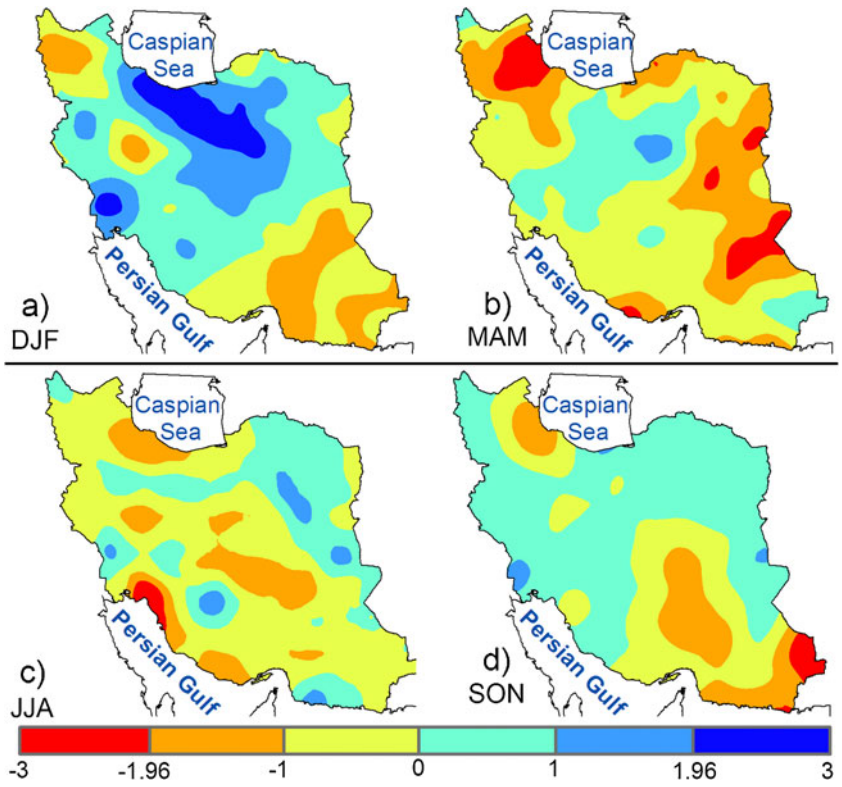

Fig. 5 Spatial pattern of Mann–Kendal trend test (Z statistics) for: **a** winter, **b** spring, **c** summer and **d** autumn precipitation over Iran. Statistically significant upward and downward trends are for $Z \geq 1.96$ and $Z \leq -1.96$, respectively

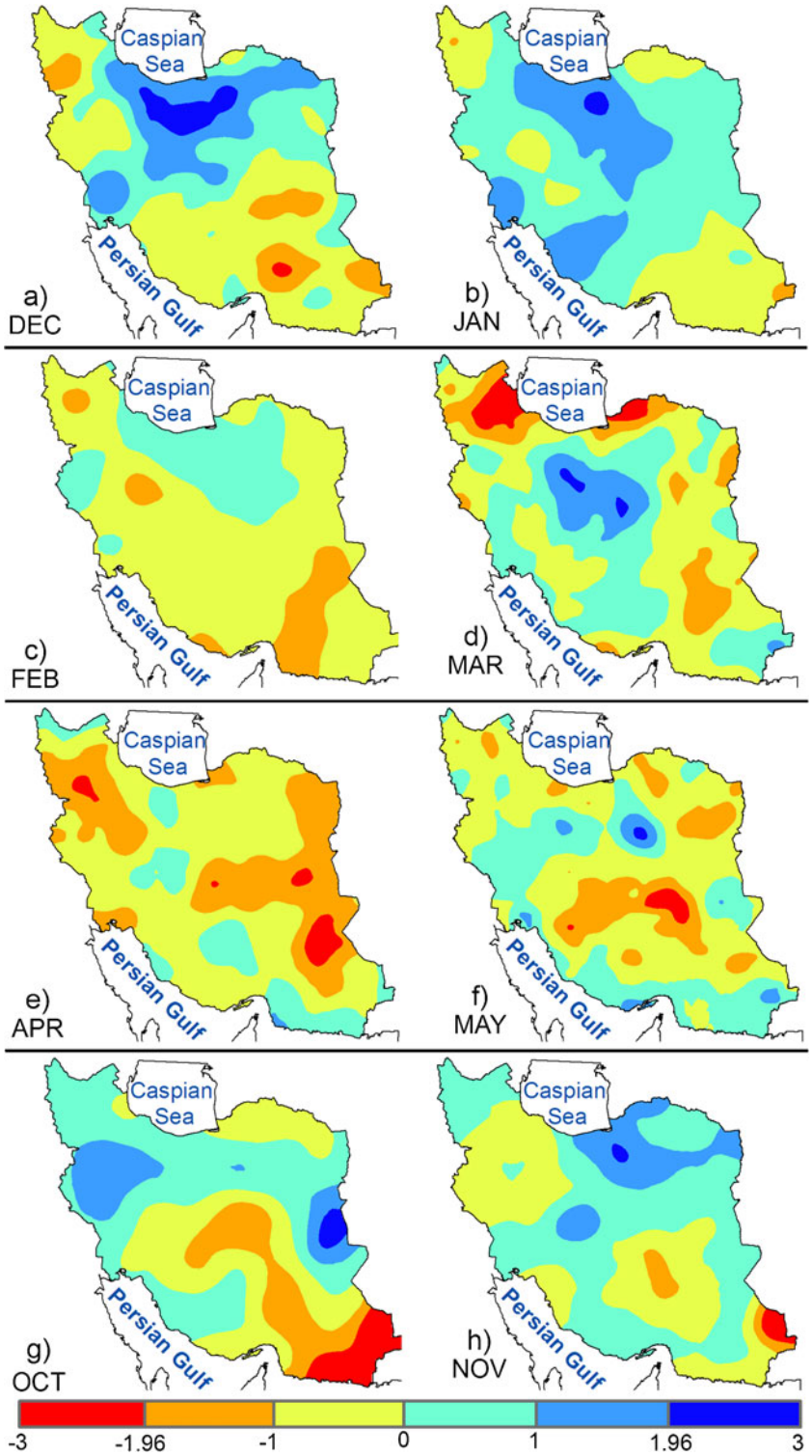

Fig. 6 Spatial pattern of Mann–Kendal trend test (Z statistics) for monthly precipitation over Iran. Statistically significant upward and downward trends are for $Z \geq 1.96$ and $Z \leq -1.96$, respectively

statistically significant downward trend. In March, central-western Iran is characterised with upward trend, but the remaining parts of the country show downward trend, which is statistically significant only in the south-western and south-eastern Caspian Sea. Precipitation trends for April and May are downward in almost the whole country, being statistically significant only in some locations in eastern and north-western Iran. Differently, upward trend dominates most parts of the country in October and November, with the exception of south-eastern Iran that exhibits statistically significant downward trend in these 2 months. Results suggest that precipitation in Iran tends to increase in central regions during the cold season in autumn and winter, leaving the warm season with less precipitation occurrences and,

therefore, intensifying the seasonality and dryness of the country.

4 Conclusions

The spatial patterns of annual, seasonal and monthly total precipitation over Iran and the corresponding long-term trends are investigated using GPCC gridded precipitation dataset with 0.5° resolution and covering the period 1951–2009. The spatial patterns of total annual, winter and spring precipitation and the associated coefficients of variations reflect the role of orography and sea neighbourhood in determining the differences in precipitation between central arid and semi-arid areas and northern and western mountainous regions. The highest annual precipitation amount is observed in the Caspian Sea region and mountainous areas of northern and western Iran, and the lowest is observed in the central, eastern and southern Iran. The spatial variability of PCI also shows the substantial differences between northern and southern Iran in the distribution of precipitation within the year, suggesting that the northern and western mountainous areas have relatively regular precipitation distribution during the year, whereas southern areas are characterised by a strongly marked seasonality. Summer and autumn are very dry seasons, particularly in central, eastern and southern Iran. In both seasons, the highest precipitation is observed in mountainous areas of Alborz and in the Caspian Sea region. The spatial pattern of precipitation in December, January, February and March are very similar to the pattern of winter and annual precipitation, showing the highest precipitation amount in western mountainous areas and the lowest in the central, eastern and southern Iran. However, the precipitation occurrences retreated rapidly from south to north from April to September, being limited to the Caspian Sea region in August and September.

The spatial distribution of MK trends for total annual precipitation showed downward trends in north-western and south-eastern Iran, whereas western, central and north-eastern Iran is characterised by upward trends. However, the observed downward/upward trends are statistically significant only in some limited regions. The spatial patterns of MK trend test for each season revealed that the winter and autumn precipitation increased in most parts of Iran, particularly in northern areas, where the trend is statistically significant. Differently, a not statistically significant downward trend was identified in north-western and south-eastern Iran. On the contrary, the spring precipitation showed downward trend in most of the country that is statistically significant only in north-western and eastern Iran. The spatial pattern of MK trend for JJA also revealed a not statistically significant downward trend in most of the country. Upward trend was observed in north-eastern Iran.

It was found that the precipitation in December tends to increase in central-northern Iran and decrease in south and north-western country. In January, approximately the whole country exhibited upward trend, with the exception of some locations in south-eastern, north-western and north-eastern Iran. In February, March, April and May, not statistically significant downward trend was observed with the exception of some locations where upward trend was found. Differently, an upward trend was identified in most of Iran during October and November, with the exception of south-eastern country that exhibited statistically significant downward trend in these two months.

In summary, precipitation in winter and autumn showed upward trend in most of Iran, with the exception of north-western and south-eastern Iran, where the observed trend is downward in both seasons. On the contrary, the country is mostly characterised by downward trend in spring and summer, with the exception of limited areas in central and north-eastern Iran showing upward trend. Thus, using the GPCC dataset it has been found that precipitation tends to decrease during the warm seasons (spring and summer) and increase during cold seasons (autumn and winter) in most of Iran. This would imply less precipitation occurrences during the warm season and an intensification of the seasonality and dryness over the country; nevertheless, the north-western and south-eastern regions show to have downward trends also during the cold seasons, though not statistically significant.

Acknowledgement The GPCC data were freely provided by the Deutscher Wetterdienst through their Web site http://www.dwd.de.

References

da Silva VPR (2004) On climate variability in northeast of Brazil. J Arid Environ 58:575–596

De Luis M, Raventos J, Gonzales-Hidalgo JC, Sanchez JR, Cortina J (2000) Spatial analysis of rainfall trends in the region of Valencia (East Spain). Int J Climatol 20:1451–1469

Dinpashoh Y, Fakheri-Fard A, Moghaddam M, Jahanbakhsh S, Mirnia M (2004) Selection of variables for the purpose of regionalization of Iran's precipitation climate using multivariate methods. J Hydrol 297:109–123

Domroes M, Kaviani M, Schaefer D (1998) An analysis of regional and intra-annual precipitation variability over Iran using multivariate statistical methods. Theor Appl Climatol 61:151–159

Gong DY, Shi PJ, Wang JA (2004) Daily precipitation changes in the semi-arid region over northern China. J Arid Environ 59:771–784

González Hidalgo JC, De Luís M, Raventós J, Sánchez JR (2003) Daily rainfall trend in the Valencia Region of Spain. Theor Appl Climatol 75:117–130

IPCC (2007) Climate change: synthesis report of the fourth assessment report. IPCC, Geneva

Lettenmaier DP, Wood EF, Wallis JR (1994) Hydro-climatological trend in the continental United States, 1948–88. J Clim 7:586–607

Modarres R, Sarhadi A (2009) Rainfall trends analysis of Iran in the last half of the twentieth century. J Geophys Res 114, D03101. doi:10.1029/2008JD010707

Modarres R, da Silva VPR (2007) Rainfall trends in arid and semi-arid regions of Iran. J Arid Environ 70:344–355

Partal T, Kahya E (2006) Trend analysis in Turkish precipitation data. Hydrol Process 20:2011–2026

Raziei T, Daneshkar Arasteh P, Saghafian B (2005) Annual rainfall trend in arid and semi arid region of Iran. In: Dannowski R (ed) Integrated land and water management: towards sustainable rural development (Proc. ICID 21st European Reg. Conf., Frankfurt (Oder), Germany, and Słubice, Poland), ICID German Nat. Com., Münchberg, CD-ROM

Raziei T, Bordi I, Pereira LS (2008) A precipitation-based regionalization for Western Iran and regional drought variability. Hydrol Earth Syst Sci 12:1309–1321

Raziei T, Bordi I, Pereira LS, Sutera A (2010) Space-time variability of hydrological drought and wetness in Iran using NCEP/NCAR and GPCC datasets. Hydrol Earth Syst Sci 14:1919–1930

Raziei T, Bordi I, Pereira LS (2011) An application of GPCC and NCEP/NCAR datasets for drought variability analysis in Iran. Water Resour Manage 25:1075–1086

Raziei T, Mofidi A, Santos JA, Bordi B (2012) Spatial patterns and regimes of daily precipitation in Iran in relation to large-scale atmospheric circulation. Int J Climatol 32:1226–1237

Schneider U, Fuchs T, Meyer-Christoffer A et al (2008) Global precipitation analysis products of the GPCC, Global Precipitation Climatology Centre (GPCC), DWD, Internet Publication. (http://www.dwd.de), 1–12

Soltani S, Modarres R, Eslamian SS (2007) The use of time series modelling for the determination of rainfall climates of Iran. Int J Climatol 27:819–829

Tabari H, Hosseinzadeh Talaee P (2011) Temporal variability of precipitation over Iran: 1966–2005. J Hydrol 396:313–320

Turkes M (1996) Spatial and temporal analysis of annual rainfall variations in Turkey. Int J Climatol 16:1057–1076

Willmott CJ, Rowe CM, Philpot WD (1985) Small-scale climate maps: a sensitivity analysis of some common assumptions associated with grid-point interpolation and contouring. Am Cartogr 12:5–16

Xu ZX, Tkeuchi K, Ishidaria H (2003) Monotonic trend and step changes in Japanese precipitation. J Hydrol 279:144–150

Yatagai A, Xie P, Alpert P (2008) Development of a daily gridded precipitation data set for the Middle East. Adv Geosci 12:165–170

Yatagai A, Arakawa O, Kamiguchi K, Kawamoto H, Nodzu MI, Hamada A (2009) A 44-year daily gridded precipitation dataset for Asia based on a dense network of rain gauges. SOLA 5:137–140

Zhang X, Vincent LA, Hogg WD, Niitsoo A (2000) Temperature and precipitation trends in Canada during the 20th century. Atmos Ocean 38:395–429